Bull. Chem. Soc. Ethiop. **2025**, 39(2), 327-339.
DOI: https://dx.doi.org/10.4314/bcse.v39i2.11

ISSN 1011-3924
Printed in Ethiopia
Online ISSN 1726-801X

COMPLEXES OF THE ANTIBIOTIC DRUG SUCCINYLSULFATHIAZOLE WITH THE La(III), Sm(III), and Tb(III) IONS: SPECTRAL CHARACTERIZATIONS, MICROSCOPIC PICTURES, AND THERMAL PROPERTIES

Abdulrahman A. Almehizia[1*], Hamad M. Alkahtani[2], Amer Alhaj Zen[3], Ahmad J. Obaidullah[2], Ahmed M. Naglah[1**], Moayad M. Alzughaibi[4] and Hala H. Eldaroti[5]

[1]Drug Exploration and Development Chair (DEDC), Department of Pharmaceutical Chemistry, College of Pharmacy, King Saud University, P.O. Box 2457, Riyadh 11451, Saudi Arabia
[2]Department of Pharmaceutical Chemistry, College of Pharmacy, King Saud University, P.O. Box 2457, Riyadh 11451, Saudi Arabia
[3]Chemistry & Forensics Department, Clifton Campus, Nottingham Trent University, Nottingham Ng11 8NS, UK
[4]Chemistry Department, Faculty of Science and Art, Al-Baha University, Mukhwah Branch, Al-Baha 65731, Saudi Arabia
[5]Department of Chemistry, Faculty of Education, Alzaeim Alazhari University, Khartoum, Sudan

(Received September 25, 2024; Revised November 5, 2024; Accepted November 7, 2024)

ABSTRACT. Reacting the antibiotic drug succinylsulfathiazole (abbreviated as SST) with the lanthanide metal ions La(III), Sm(III), and Tb(III) generated thermal stable metal-based complexes. The temperature of the reaction was 70 ºC, at a pH of ~ 8.5, using stoichiometry of 2:1 (SST ligand to metal ion). Spectral and analytical characterizations of the SST metal-based complexes were obtained using ultraviolet/visible (UV-visible), Fourier-transform infrared (FT-IR) spectroscopies, X-ray diffractometry (XRD), and CHN elemental analysis. The microscopic pictures of the SST complexes were captured by a high-resolution scanning electron microscope with environmental mode (ESEM). Experimental data suggested that the general composition of La(III) complex is $[La(SST)_2(H_2O)Cl].6H_2O$ with a gross formula of $C_{26}H_{38}N_6O_{17}S_4ClLa$, the general composition of Sm(III) complex is $[Sm(SST)_2(H_2O)(NO_3)].5H_2O$ with a gross formula of $C_{26}H_{36}N_7O19S_4Sm$, whereas the general composition of Tb(III) complex is $[Tb(SST)_2(H_2O)(NO_3)].4H_2O$ with a gross formula of $C_{26}H_{34}N_7O_{18}S_4Tb$. In the manufactured complexes, two deprotonated SST molecules were captured the La(III), Sm(III), and Tb(III) ions by their bidentate carboxylate groups (COO^-). The microscopic pictures clearly revealed different surface topography between SST metal-based complexes.

KEY WORDS: Succinylsulfathiazole, Lanthanides, SEM, Surface morphology, EDS profile

INTRODUCTION

The term antibiotic refers to any substance that possesses biological activity towards living organisms. These biological activities are antiparasitic, antifungal, and antibacterial activity. Antibiotics have various effects on living organisms, ranging from inhibiting their metabolic activity (bacteriostatic) to causing their death (bactericides). Today, numerous different kinds of antibiotics are widely used in the world, not only to treat and prevent human infections but also in animals and plants. One kind of antibiotic that has been in clinical use since 1968 is sulfonamides. Sulfonamides are synthetic antimicrobial agents used to treat many human infectious diseases, such as ear infections, upper respiratory tract infections and urinary tract infections [1]. Sulfonamides are weak acid organic compounds soluble in water, and after

*Corresponding authors. E-mail: mehizia@ksu.edu.sa; anaglah@ksu.edu.sa

releasing them into the environment, they run off into surface water and groundwater. The occurrence of antibiotics in the environment may promote resistance in clinically relevant microorganisms, leading to a potential threat to the effectiveness of antibiotic therapies.

The complexation of metal ions with natural and biologically active molecules plays an important role in biology, chemistry, pharmacology, and medicine. The resulting products from this complexation, known as metallodrugs or metal-based drugs, exhibit a wide range of medical and pharmaceutical applications [2-15]. Over the years, numerous metal-based drugs have demonstrated their potential biological profiles (i.e., antibacterial, anticancer, and antiviral properties) [16-18]. Studying the chemical reactions between metal ions and bio-active molecules has several benefits: (i) Improving the biological profiles of several biologically active molecules and drugs. (ii) Discovering novel bio-active metal-based complexes with potential biological properties to treat new diseases such as coronavirus disease (COVID-19). (iii) Reducing the rate of drug resistance. (iv) Overcome severe adverse side effects of current metallodrugs.

This work aims to explore the complexation property of one member of sulfonamide antibiotics, succinylsulfathiazole (Figure 1; abbreviated as SST), towards three of the lanthanide metal ions [La(III), Sm(III), and Tb(III)]. These metal ions were reacted with the SST ligand at a temperature of 70 °C, at a pH of ~ 8.5 using 1:2 (metal ion to SST ligand) stoichiometry. The separation and purification of the manufactured metal-base complexes were carried out with meticulous care, and they were characterized by several physicochemical techniques.

EXPERIMENTAL

Materials

Lanthanum(III) chloride heptahydrate ($LaCl_3 \cdot 7H_2O$; 371.37 g/mol), samarium nitrate hexahydrate ($Sm(NO_3)_3 \cdot 6H_2O$; 444.47 g/mol), and terbium(III) nitrate pentahydrate ($Tb(NO_3)_3 \cdot 5H_2O$; 435.02 g/mol) were the lanthanide metal ions used in this work and were provided by Sigma-Aldrich (St Louis, MO, USA) in high purity (99.99%). The ligand in this work was succinylsulfathiazole (SST; $C_{13}H_{13}N_3O_5S_2$; 355.38 g/mol) was purchased from Merck Chemical Company (KGaA, Germany).

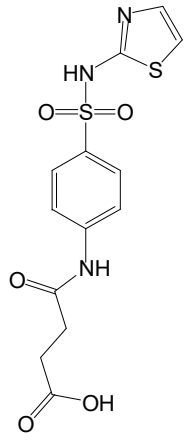

Figure 1. Chemical structure of the SST molecule.

Characterization techniques

A Shimadzu Fourier-transform infrared spectrophotometer collected the FT-IR spectra (4000-400 cm^{-1}). A Perkin-Elmer Lambda 25 UV/Vis spectrophotometer collected the electronic absorption spectra (200-800 nm). An X'Pert Philips X-ray diffractometer was used to collect the XRD diffractograms (2θ 10°-80°). A Cu Ka1 was used as an X-ray source with λ = 0.154056 nm. A Perkin-Elmer 2400 series II CHN elemental analyzer was used to obtain the relative elemental compositions (C%, H%, N%). A high-resolution SEM with environmental mode (Quattro ESEM; Thermo Fisher Scientific) integrated with an energy-dispersive X-ray spectroscopy (EDS) was used to capture the microscopic pictures and record the EDS profiles, showcasing the latest in microscopy technology.

Synthesis of SST complexes

Complexes of SST ligand with La(III), Sm(III), and Tb(III) ions were synthesized as follows: Three portions of SST methanolic solutions were prepared by dissolving 2 mmol of SST in 25 mL methanol. The SST solutions were hated on hot plate with a magnetic stirrer at 70 °C for a few minutes. Aqueous solutions of La(III), Sm(III), and Tb(III) ions containing 1 mmol in 25 mL were gradually added severally to the SST solutions. The pH of the three solutions was bringing to approximately ~ 8.5 using a few drops of 5% NH_3. Stirring the La-SST, Sm-SST, and Tb-SST solutions for an additional 15 min led to the beginning of the formation of colored precipitates. To ensure complete precipitation of La(III), Sm(III), and Tb(III) complexes, their beakers were left overnight. The products were collected from the reaction vessels by filtration, and the unreacted starting materials were removed by washing the products thoroughly with hot deionized water, diethyl ether, and methanol. The purified products were oven dried at 70 ºC, and then stored in a vacuum desiccator.

RESULTS AND DISCUSSIONS

Analytical and electronic spectral data

The SST ligand was dissolved in methanol solvent, where La(III), Sm(III), and Tb(III) salts were dissolved in Milli-Q purified water. La-SST, Sm-SST, and Tb-SST complexes were collected at 70 °C, at pH of ~ 8.5, using stoichiometry of 1:2 (metal ion to SST ligand). The manufactured metal-based complexes were soluble in *N*,*N*-dimethylformamide (DMF) and dimethyl sulfoxide (DMSO) solvents, and insoluble in water and most organic solvents. In these complexes, metal (La, Sm, Tb) and water were determined gravimetrically, where the contents of C, N, S and H elements were measured by CHNS elemental analyzer. Table 1 lists the percentage (%) of C, N, S, H, metal, and water in the manufactured metal-based complexes.

Table 1. The percentage (%) of C, N, S, H, metal, and water in the manufactured metal-based complexes.

Complex	Results											
	Found (%)						Calculated (%)					
	C	N	S	H	Metal	H_2O	C	N	S	H	Metal	H_2O
La(III)	31.15	8.60	12.56	3.94	13.65	12.33	30.92	8.33	12.68	3.76	13.76	12.49
Sm(III)	30.50	9.73	12.19	3.70	14.44	10.37	30.32	9.52	12.43	3.50	14.61	10.49
Tb(III)	30.38	9.50	12.32	3.48	15.60	9.05	30.60	9.61	12.55	3.33	15.58	8.83

Data presented in Table 1 suggest that the reaction stoichiometry between SST ligand and the investigated metal ions was 2:1 (SST ligand: metal), revealing that the complexes of La(III), Sm(III), and Tb(III) ions were formulated as $[La(SST)_2(H_2O)Cl]\cdot 6H_2O$,

$[Sm(SST)_2(H_2O)(NO_3)]\cdot 5H_2O$, $[Tb(SST)_2(H_2O)(NO_3)]\cdot 4H_2O$, respectively. The corresponding gross formulas are $C_{26}H_{38}N_6O_{17}S_4ClLa$ (1009.11 g/mol), $C_{26}H_{36}N_7O_{19}S_4Sm$ (1029.12 g/mol), and $C_{26}H_{34}N_7O_{18}S_4Tb$ (1019.68 g/mol), respectively. The DMSO solutions of La(III), Sm(III), and Tb(III) complexes were scanned by a UV/Vis spectrophotometer, and the obtained spectra are illustrated in Figure 2. The UV-visible spectrum of La(III) complexes was characterized by two weak and broad absorption bands at 206 and 290 nm. Two very strong and sharp absorption bands with approximately the same intensity and width. The two bands appeared at 240 and 255 nm. The band at 240 nm had a shoulder band with medium intensity centered at 230 nm. Two weak and broad absorption bands characterized the UV-Visible spectrum of Sm(III) complexes, appearing at 206 and 290 nm. A twin absorption band is located at 220 and 230 nm. An intense and sharp absorption band is centered at 255 nm. The intensity and width of this band are slightly higher than those of the twin bands.

The UV-Visible spectrum of Tb(III) complexes was characterized by two weak and broad absorption bands accumulated at 260 and 288 nm. The band at 288 nm is broader than that at 260 nm. A twin absorption band is located at 220 and 230 nm. Intense and sharp absorption bands centered at 245 nm. All these absorption bands may be assignable to the $\pi \rightarrow \pi^*$ transitions.

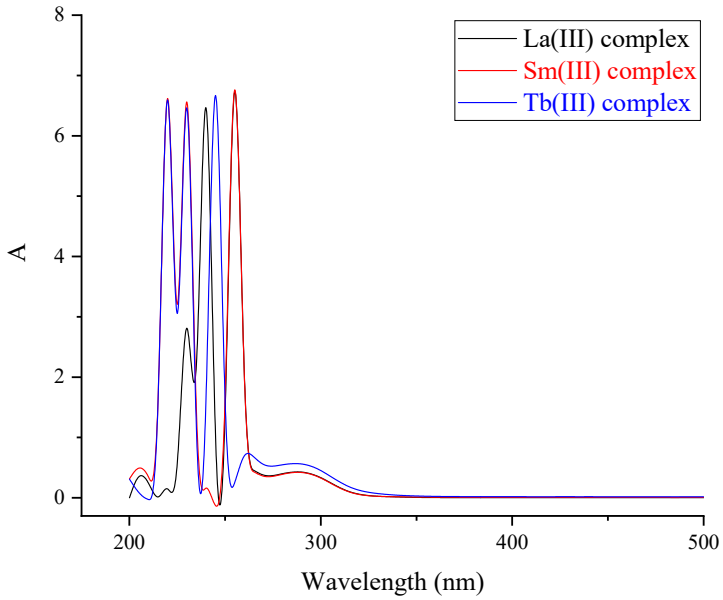

Figure 2. UV-visible spectra of the manufactured La(III), Sm(III), and Tb(III) complexes.

FT-IR spectral data

The important FTIR spectral bands of the free SST ligand and its metal complexes with La(III), Sm(III), and Tb(III) ions were listed in Table 2. The free SST ligand has many different functional groups: O–H, C=O (carboxylic), C=O (carbonyl), $-SO_2$, C=C (aromatic), C=N, C–N, –NH, –N–S–, and –C–S–. These functional groups produced several vibrational modes. Band appeared at 3494 cm^{-1} was attributed to the ν(O–H) vibrations of the –COOH group. Bands located at 1402, 1220, and 633 cm^{-1} could be assigned to the vibrations of δ_{def}(O–H), δ(O–H) in-plane bending, and

δ(O–H) out-of-plane bending, respectively. The vibrations of $\nu(C{=}O)_{COOH}$ and $\nu(C{=}O)_{CONH}$ generated to strong bands at 1701 and 1675 cm^{-1}, respectively. The C–H of phenyl ring, 1,3-thiazole ring, and $–CH_2$ groups generated multiple absorption bands located at 2924 cm^{-1} ν_{as}(C–H), 2854 cm^{-1} ν_s(C–H), 1432 cm^{-1} δ_{def}(C–H), 1295 cm^{-1} δ_{def}(C–H), 1250 cm^{-1} $\delta_{rock}(CH_2)$, 949 cm^{-1} $\delta_{wag}(CH_2)$, 864 cm^{-1} δ_{def}(C–H), 701 δ_{def}(C–H), 653 cm^{-1} $\delta_{rock}(CH_2)$, and 504 cm^{-1} $\delta_{twist}(CH_2)$ [19]. The bands resonated at 3333 and 3101 cm^{-1} were assigned to the ν(N–H) vibrations. The $–SO_2$ group originated four absorption bands at 1376, 1185, 568, and 555 cm^{-1} resulted from the $\nu_{as}(SO_2)$, $\nu_s(SO_2)$, $\delta_{sciss}(SO_2)$, and $\delta_{wag}(SO_2)$, vibrations, respectively. Bands located at 1596 and 1539 could be attributed to the ν(C=N) mode of 1,3-thiazole nitrogen and ν(C=C) mode, respectively [19].

After the complexation between SST and the investigated metal ions, the absorption band resulted from the $\nu(C{=}O)_{COOH}$ vibrations, which resonated at 1701 cm^{-1} in the free ligand, was no longer observed in the FTIR spectra of the complexes. Two new absorption bands were detected at 1565, 1567 and 1566 cm^{-1} for La(III), Sm(III), and Tb(III) complexes, respectively resulted from the $\nu_{as}(COO^-)$ mode, and at 1450, 1440 and 1447 cm^{-1}, respectively resulted from the $\nu_s(COO^-)$ mode of the carboxylate group. The bands resulted from the ν(N–H) and ν(CONH) vibrations were remains un shifted or slightly shifted, propose that N–H and –CONH groups were not participating in the chelation process between SST ligand and La(III), Sm(III), and ion. The bands resulted from the $\nu_{as}(SO_2)$ and $\nu_s(SO_2)$ vibrations were slightly shifted. Bands due to the $\nu_{as}(SO_2)$ vibrations were appeared at 1375, 1372, an 1374 cm^{-1} in the IR spectra of La(III), Sm(III) and Tb(III) complexes, respectively, where bands due to the $\nu_s(SO_2)$ vibrations were detected at 1175, 1172, and 1177 cm^{-1}, respectively. The scissoring and waging vibrations of $–SO_2$ were located at (562 and 560 cm^{-1}), (567 and 558 cm^{-1}), and (570 and 559 cm^{-1}) in the IR spectra of La(III), Sm(III) and Tb(III) complexes, respectively. The IR spectra of La(III), Sm(III), and Tb(III) complexes contain new medium-intensity absorption bands at 446, 452, and 453 cm^{-1}, respectively. These bands could be assigned to the stretching vibrations of La–O, Sm–O, and Tb–O bonds, respectively. The IR spectral data proposed that the SST ligand captured the La(III), Sm(III), and Tb(III) ions by the bidentate carboxylate group (COO^-) [20]. Based on the analytical and FT-IR spectral data, proposed chemical structures of the La(III), Sm(III), and Tb(III) complexes were presented in Figure 3.

XRD spectral data

The XRD measurements for La(III), Sm(III), and Tb(III) complexes were performed by scanning the synthesized complexes by an XRD instrument in the 2θ range of 10-80°. The XRD diffraction patterns collected were used to drive the spectral data of the strongest three peaks which are listed in Table 3. The XRD diffractogram of La(III) complex was characterized by a single, robust, intense, and sharp diffraction peak at Bragg's angle 2θ 32.7567°. Two diffraction peaks with low-intensity were also observed in the spectrum of La(III) complex centered at 21.0598° and 23.0550°. Five diffraction peaks were observed in the XRD spectrum of Sm(III) complex in the range from 18° to 30°. These peaks were located exactly at 2θ 19.6036° (very strong), 21.9357° (medium), 24.4507° (medium), 25.8174° (strong), and 29.0766° (medium). The XRD patterns of Sm(III) complex suggest that it mainly possess an amorphous morphology. Only three reflections were observed in the XRD spectrum of Tb(III) complex, reflecting that this complex had a well-crystallized and well-defined morphology. These reflections appeared at Bragg's angle 2θ values of 22.6559° (very strong), 29.0424° (very strong), and 33.0595° (medium). The full width at half-maximum (FWHM) of the most robust diffraction peak was found to be 0.49710°, 0.61910°, and 1.26660° for La(III), Sm(III), and Tb(III) complex, respectively. Value of the inter-planar spacing between the atoms (*d*-spacing) was obtained based on the most intense peak in the complexes'

XRD diffractogram, and it was found to be 2.73176 Å, 4.52478 Å, and 3.92161 Å for La(III), Sm(III), and Tb(III) complex, respectively.

Table 2. The important FTIR spectral bands (cm^{-1}) of the free SST ligand and its metal complexes with La(III), Sm(III), and Tb(III) ions.

Free SST	Complexes			Assignments
	La(III)	Sm(III)	Tb(III)	
3494	-	-	-	ν(O–H); COOH
3333	3325	3327	3300	ν(N–H); amide
3101	3115	3103	3105	ν(N–H)
2924, 2854	2913, 2806	3044	2910	ν_s(C–H) + ν_{as}(C–H)
1701	-	-	-	ν(C=O); COOH
1675	1678	1672	1670	ν(CONH)
1596	1589	1591	1587	ν(C=N)
-	1565	1567	1566	$\nu_{as}(COO^-)$
1539	1527	1522	1524	ν(C=C); aromatic ring
1497	-	1500	-	$\delta_{sciss}(CH_2)$
-	1450	1440	1447	$\nu_s(COO^-)$
1432	1436	-	1432	δ_{def}(C–H)
1402	1403	1400	1399	δ_{def}(O–H)
1376	1375	1372	1374	$\nu_{as}(SO_2)$
1317	1320	1323	-	ν_{as}(C–N)
1295	1303	1305	1305	δ_{def}(C–H)
1250	1260	-	1267	$\delta_{rock}(CH_2)$
1220	-	-	1218	δ(O–H) in-plane bending
1185	1175	1172	1177	$\nu_s(SO_2)$
1146	1139	1139	1134	ν(C–O)
1126	-	1130	1135	ν_s(C–N)
1092, 1016	1086, 1012	1087, 1039	1087, 1015	Ring breathing vibrations
949	935	930	932	$\delta_{wag}(CH_2)$
864	889	892	-	δ_{def}(C–H)
839	842	831	830	ν(S–N)
745	-	750	731	ν(C–S)
701	705	717	705	δ_{def}(C–H)
653	-	675	-	$\delta_{rock}(CH_2)$
633	639	640	635	δ(O–H) out-of-plane bending
568	562	567	570	$\delta_{sciss}(SO_2)$
555	560	558	559	$\delta_{wag}(SO_2)$
504	507	504	505	$\delta_{twist}(CH_2)$
-	446	452	453	ν(M–O)

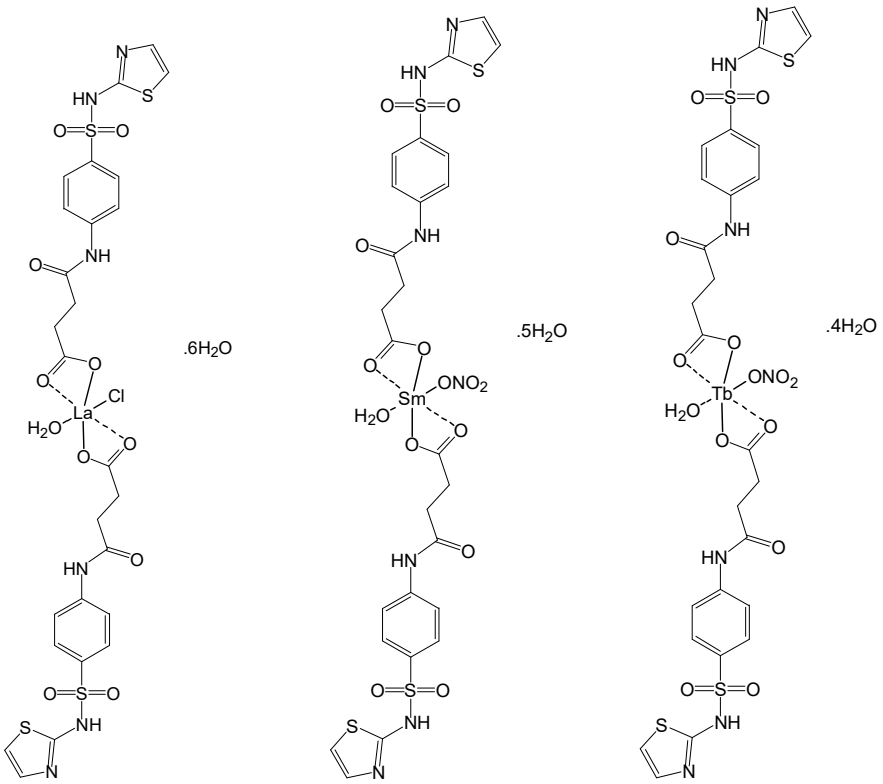

Figure 3. Proposed chemical structures of the La(III), Sm(III), and Tb(III) complexes.

Table 3. The XRD spectral data of the strongest three peaks for the synthesized La(III), Sm(III), and Tb(III) complexes.

Complex	XRD data					
	Peak no.	2θ (deg)	*d*-spacing value; (Å)	Intensity (I/I1)	FWHM (deg)	Intensity (counts)
La(III) complex	21	32.7567	2.73176	100	0.49710	418
	13	23.0550	3.85462	45	0.00000	189
	11	21.0598	4.21508	33	0.96580	137
Sm(III) complex	7	19.6036	4.52478	100	0.61910	144
	12	25.8174	3.44810	81	0.97560	117
	11	24.4507	3.63766	75	1.15830	108
Tb(III) complex	5	22.6559	3.92161	100	1.26660	320
	8	29.0424	3.07213	97	0.66370	309
	10	33.0595	2.70743	69	0.68060	222

Microscopic pictures and EDS profiles

A high-resolution ESEM with environmental mode integrated with an energy dispersive X-ray spectroscopy (EDS) was used to capture the microscopic pictures and record the EDS profiles for

the manufactured SST metal-based complexes. The microscopic pictures presented in Figure 4 revealed clearly different surface topography between SST metal-based complexes. The particles of La(III) complex scattered small pieces, and these pieces had different sizes and shapes. The surface of La(III) particles is rough. Some of these pieces were accumulated together and form big agglomerates. The complexation of SST with Sm(III) ions led to a cotton-like shaped morphology. Among SST complexes, the particles of Tb(III) complex had a well-homogeneous, clear feature, and well-defined shape. The particles of Tb(III) complex had a large and well smooth plate-like morphology. This surface topography contributed to their large surface area. Upon magnification (×20,000), small holes were observed on the plate's surface. The EDS profiles of La(III), Sm(III) and Tb(III) complexes are illustrated in Figures 5, 6, and 7, respectively. The EDS spectrum of the La(III) complex evidenced the presence of C, O, N, S, and La elements, the EDS spectrum of the Sm(III) complex evidenced the presence of C, O, N, S, and Sm elements, and the EDS spectrum of the Tb(III) complex evidenced the presence of C, O, N, S, and Tb elements.

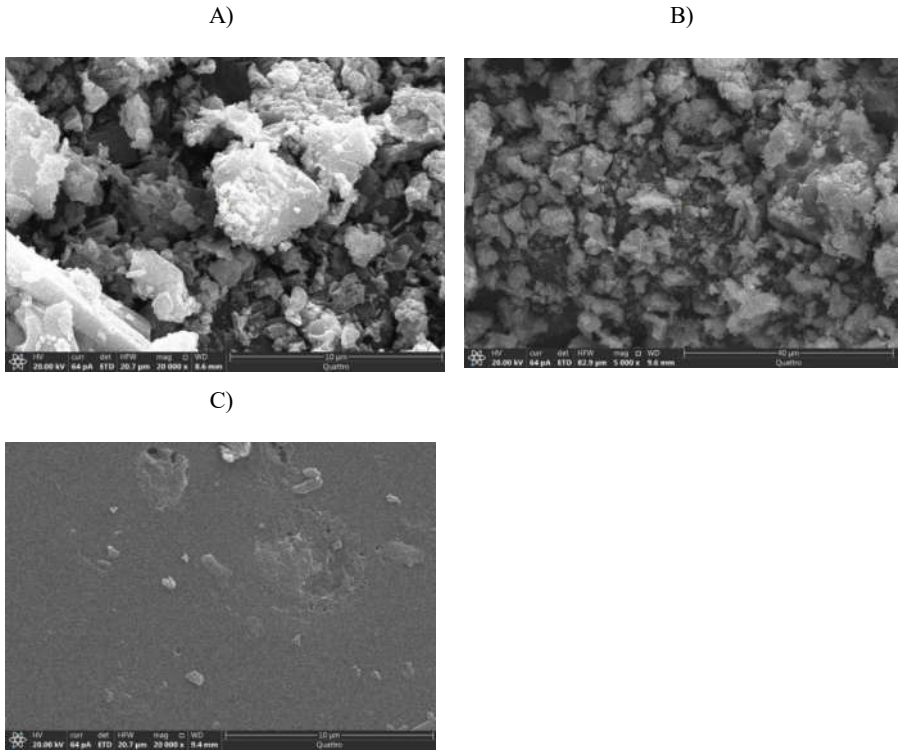

Figure 4. SEM pictures of A) La(III) complex, B) Sm(III) complex, and C) Tb(III) complex.

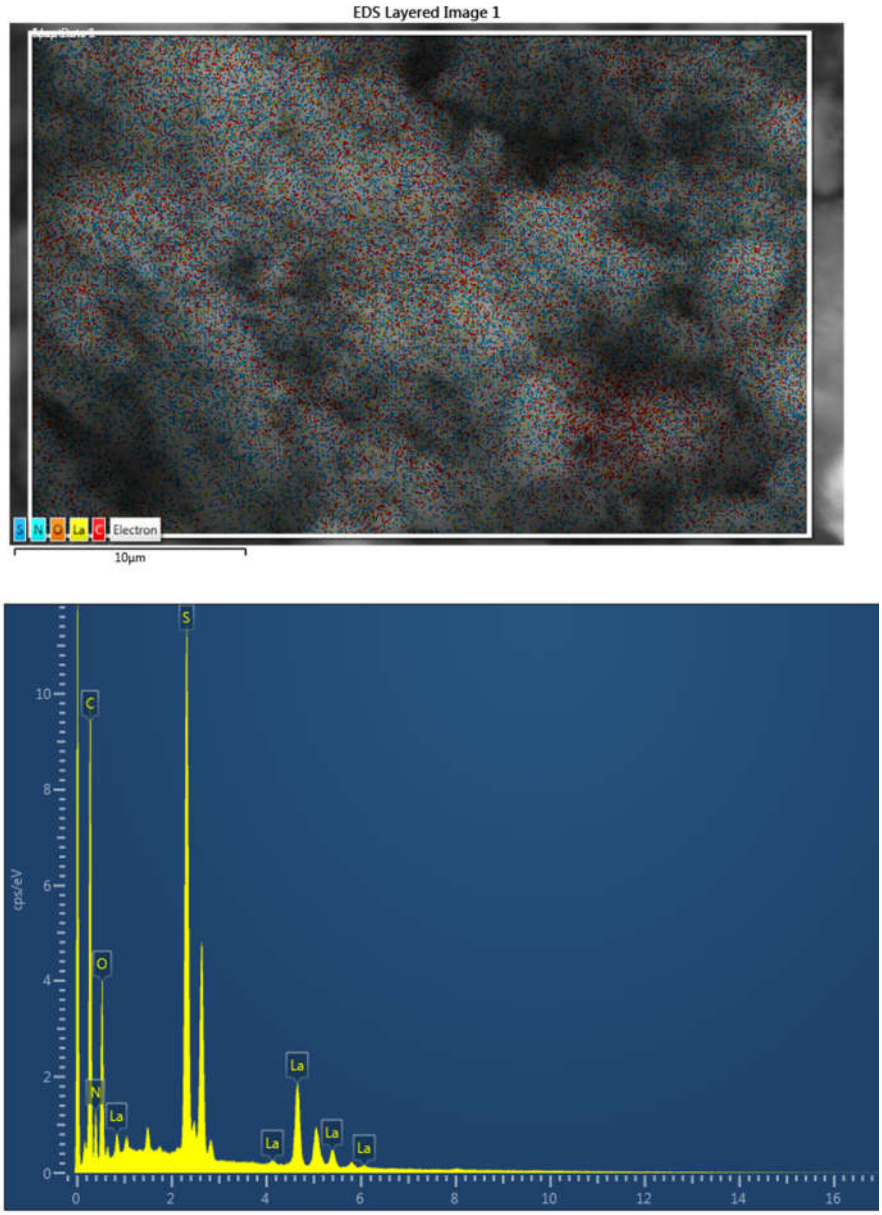

Figure 5. EDS data of La(III) complex.

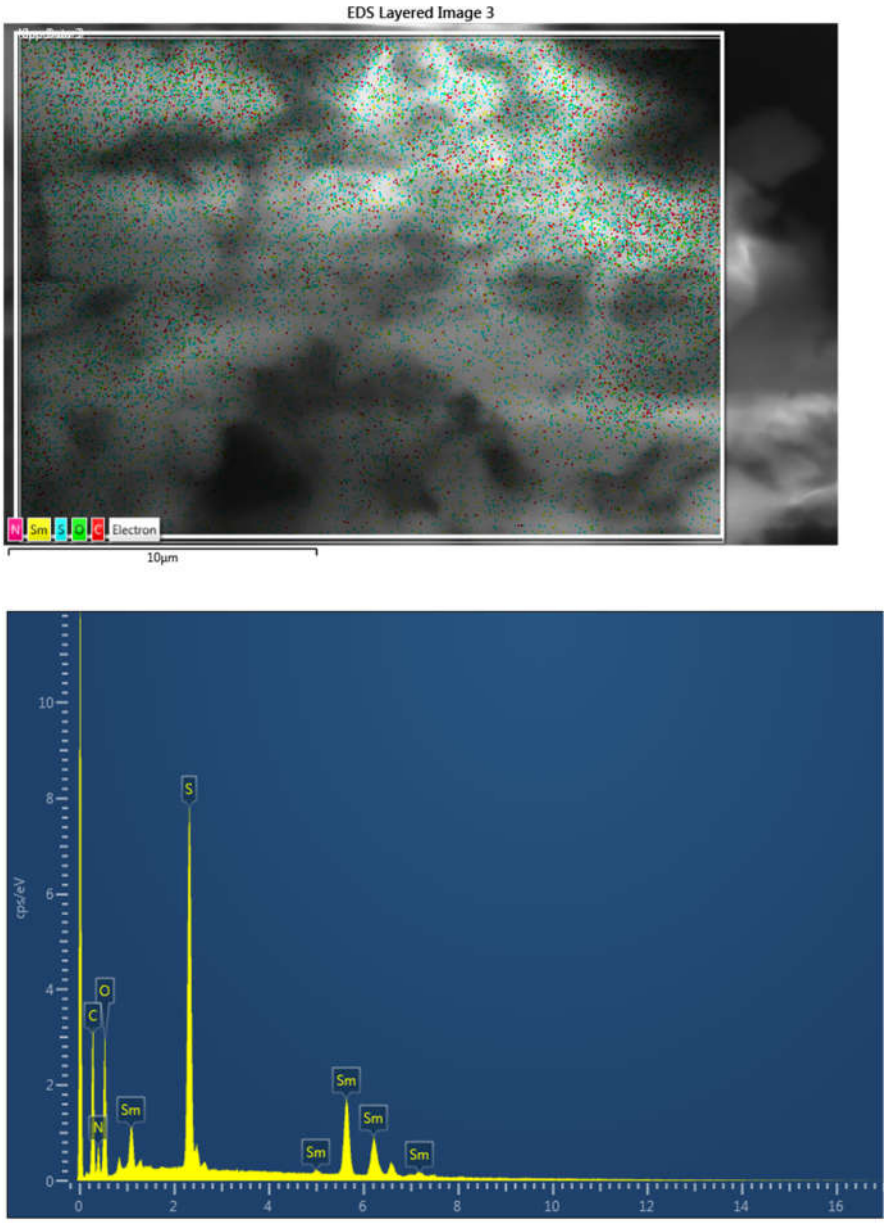

Figure 6. EDS data of Sm(III) complex.

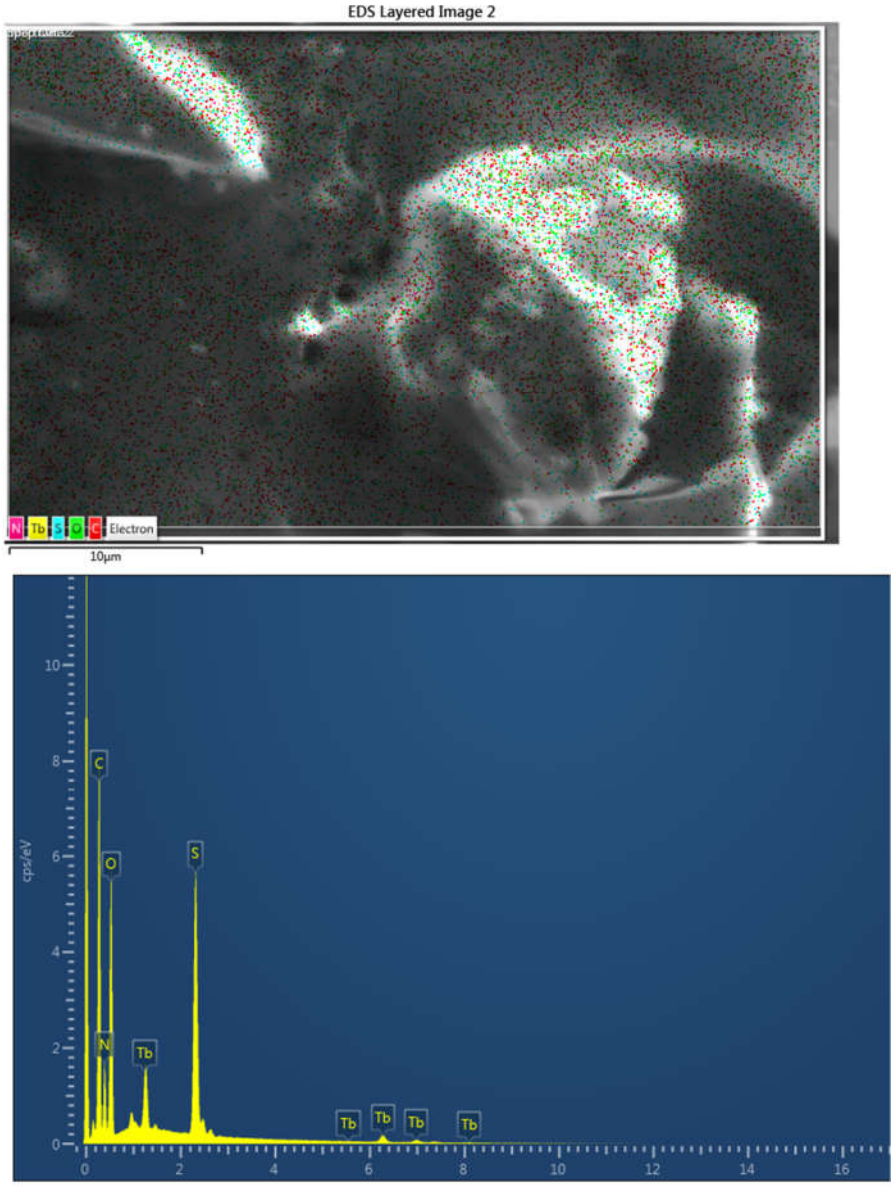

Figure 7. EDS data of Tb(III) complex.

CONCLUSION

The complexes $[La(SST)_2(H_2O)Cl]\cdot 6H_2O$, $[Sm(SST)_2(H_2O)(NO_3)]\cdot 5H_2O$, and $[Tb(SST)_2(H_2O)(NO_3)]\cdot 4H_2O$ were synthesized in a novel approach from the reaction of the antibiotic drug succinylsulfathiazole (SST) with the lanthanide metal ions La(III), Sm(III), and Tb(III). The reaction conditions were stoichiometry of 2:1 (SST ligand to metal ion), temperature of 70 °C, and pH of ~ 8.5. UV-Visible, FT-IR, XRD spectroscopies, and CHN elemental analysis characterized the formed complexes. These techniques proposed that two deprotonated SST molecules were captured, the La(III), Sm(III), and Tb(III) ions, by their bidentate carboxylate groups. The microscopic pictures of the complexes were captured by a high-resolution scanning electron microscope with environmental mode (ESEM). The captured pictures revealed different surface topography between SST complexes. Our future research will continue to explore the complex behavior of SST towards other lanthanide metal ions. This ongoing work, with its potential to expand our understanding of the chelation characteristics of SST towards lanthanide metal ions, is both inspiring and intriguing.

ACKNOWLEDGMENT

The authors extend their appreciation to the Deanship of Scientific Research, King Saud University for funding through Vice Deanship of Scientific Research Chairs; (Drug Exploration and Development Chair).

Funding

This research was funded by the Deanship of Scientific Research at King Saud University through Vice Deanship of Scientific Research Chairs; (Drug Exploration and Development Chair).

REFERENCES

1. Bag, P.P.; Kothur, R.R.; Reddy, C.M. Tautomeric preference in polymorphs and pseudopolymorphs of succinylsulfathiazole: fast, evaporation screening and thermal studies. *Cryst. Eng. Comm.* **2014**, 16, 4706-4714.
2. Alsawat, M.; Adam, A.M.A.; Refat, M.S.; Alsuhaibani, A.M.; El-Sayed, M.Y. Structural, spectroscopic, and morphological characterizations of metal-based complexes derived from the reaction of 1-phenyl-2-thiourea with Sr^{2+}, Ba^{2+}, Cr^{3+}, and Fe^{3+} ions. *Bull. Chem. Soc. Ethiop.* **2024**, 38, 1803-1814.
3. Adam, A.M.A.; Refat, M.S.; Alsuhaibani, A.M.; El-Sayed, M.Y. Preparation and characterizations of metal-based complexes derived from the reaction of trizma base with Mg(II), Ca(II), and Ba(II) ions. *Bull. Chem. Soc. Ethiop.* **2024**, 38, 1791-1801.
4. El-Habeeb, A.A.; Refat, M.S. Synthesis, spectroscopic characterizations and biological studies on gold(III), ruthenium(III) and iridium(III) complexes of trimethoprim antibiotic drug. *Bull. Chem. Soc. Ethiop.* **2024**, 38, 701-714.
5. Alsuhaibani, A.M.; Adam, A.M.A.; Refat, M.S.; Kobeasy, M.I.; Bakare, S.B.; Bushara, E.S. Spectroscopic, thermal, and anticancer investigations of new cobalt(II) and nickel(II) triazine complexes. *Bull. Chem. Soc. Ethiop.* **2023**, 37, 1151-1162.
6. Younes, A.A.O.; Refat, M.S.; Saad, H.A.; Adam, A.M.A.; Alzoghibi, O.M.; Alsulaim, G.M.; Alsuhaibani, A.M. Complexation of some alkaline earth metals with bidentate uracil ligand:

Synthesis, spectroscopic and antimicrobial analysis. *Bull. Chem. Soc. Ethiop.* **2023**, 37, 945-957.
7. Alkathiri, A.A.; Atta, A.A.; Refat, M.S.; Altalhi, T.A.; Shakya, S.; Alsawat, M.; Adam, A.M.A.; Mersal, G.A.M.; Hassanien, A.M. Preparation, spectroscopic, cyclic voltammetry and DFT/TD-DFT studies on fluorescein charge transfer complex for photonic applications. *Bull. Chem. Soc. Ethiop.* **2023**, 37, 515-532.
8. Adam, A.M.A.; Refat, M.S.; Gaber, A.; Grabchev, I. Complexation of alkaline earth metals Mg^{2+}, Ca^{2+}, Sr^{2+} and Ba^{2+} with adrenaline hormone: Synthesis, spectroscopic and antimicrobial analysis. *Bull. Chem. Soc. Ethiop.* **2023**, 37, 357-372.
9. Al-Hazmi, G.H.; Adam, A.M.A.; El-Desouky, M.G.; El-Bindary, A.A.; Alsuhaibani, A.M.; Refat, M.S. Efficient adsorption of Rhodamine B using a composite of Fe_3O_4@zif-8: Synthesis, characterization, modeling analysis, statistical physics and mechanism of interaction. *Bull. Chem. Soc. Ethiop.* **2023**, 37, 211-229.
10. Alsuhaibani, A.M.; Adam, A.M.A.; Refat, M.S. Four new tin(II), uranyl(II), vanadyl(II), and zirconyl(II) alloxan biomolecule complexes: synthesis, spectroscopic and thermal characterizations. *Bull. Chem. Soc. Ethiop.* **2022**, 36, 373-385.
11. Al-Hazmi, G.H.; Alibrahim, K.A.; Refat, M.S.; Ibrahim, O.B.; Adam, A.M.A.; Shakya, S. A new simple route for synthesis of cadmium(II), zinc(II), cobalt(II), and manganese(II) carbonates using urea as a cheap precursor and theoretical investigation. *Bull. Chem. Soc. Ethiop.* **2022**, 36, 363-372.
12. Alsuhaibani, A.M.; Refat, M.S.; Adam, A.M.A.; Kobeasy, M.I.; Kumar, D.N.; Shakya, S. Synthesis, spectroscopic characterizations and DFT studies on the metal complexes of azathioprine immunosuppressive drug. *Bull. Chem. Soc. Ethiop.* **2022**, 36, 73-84.
13. El-Sayed, M.Y.; Refat, M.S.; Altalhi, T.; Eldaroti, H.H.; Alam, K. Preparation, spectroscopic, thermal and molecular docking studies of covid-19 protease on the manganese(II), iron(III), chromium(III) and cobalt(II) creatinine complexes. *Bull. Chem. Soc. Ethiop.* **2021**, 35, 399-412.
14. Alosaimi, A.M.; Saad, H.A.; Al-Hazmi, G.H.; Refat, M.S. In situ acetonitrile/water mixed solvents: An ecofriendly synthesis and structure explanations of Cu(II), Co(II), and Ni(II) complexes of thioxoimidazolidine. *Bull. Chem. Soc. Ethiop.* **2021**, 35, 351-364.
15. Refat, M.S.; Altalhi, T.A.; Al-Hazmi, G.H.; Al-Humaidi, J.Y. Synthesis, characterization, thermal analysis and biological study of new thiophene derivative containing *o*-aminobenzoic acid ligand and its Mn(II), Cu(II) and Co(II) metal complexes. *Bull. Chem. Soc. Ethiop.* **2021**, 35, 129-140.
16. Alessio, E. *Bioinorganic Medicinal Chemistry*, Wiley-VCH Verlag GmbH and Co. KGaA; **2011**.
17. Eichhorn, G.L.; Marzilli, L.G. *Advances in Inorganic Biochemistry Models in Inorganic Chemistry*, PTR Prentice-Hall, Inc.: New Jersey; **1994**.
18. Hughes, M.N. *The Inorganic Chemistry of Biological Processes*, 2nd ed., Wiley: Chichester, England; **1984**.
19. Panicker, C.Y.; Varghese, H.T.; Georged, A.; Thomas, P.K.V. FT-IR, FT-Raman and ab-initio studies of 1,3-diphenyl thiourea. *Eur. J. Chem.* **2010**, 1, 173-178.
20. Deacon, G.B.; Phillips, R.J. Relationships between the carbon-oxygen stretching frequencies of carboxylato complexes and the type of carboxylate coordination. *Coord. Chem. Rev.* **1980**, 33, 227-250.